

Dynamic and Static Characterization of Horizontal Axis Wind Turbine Blades Using Dimensionless Analysis of Scaled-Down Models

Ahmed H. Abdulaziz*[‡], Adel M. Elsabbagh**, Wael N. Akl***

*Design and Production Engineering Department,, Faculty of Engineering, Ain Shams University, 1 Elsarayat St. Abbaseya, 11517 Cairo, Egypt

**Design and Production Engineering Department, Faculty of Engineering, Ain Shams University, 1 Elsarayat St. Abbaseya, 11517 Cairo, Egypt

***Design and Production Engineering Department, Faculty of Engineering, Ain Shams University, 1 Elsarayat St. Abbaseya, 11517 Cairo, Egypt

(ahesham@eng.asu.edu.eg, aelsabbagh@eng.asu.edu.eg, wael.akl@eng.asu.edu.eg)

[‡] Ahmed H. Abdulaziz, 1 Elsarayat St. Abbaseya, 11517 Cairo, Tel: +202 26828114,

Fax: +202 26828114, ahesham@eng.asu.edu.eg

Received: 07.01.2015 Accepted: 26.02.2015

Abstract- The blade is the most important part of the horizontal axis wind turbine. As significant as its role in the efficient function of the turbine, stands the accurate predictions of static and dynamic performances of blades during the design phase for further developments. The objective of the current research is to develop a reliable approach, in which measurements and analysis of a scaled-down model can be used to predict the performance of full-scale wind turbine blades. The Buckingham π -Theorem has been applied to develop such approach. Two cases of the scaled-down models were investigated. The first case was a 0.3 m long adequate scaled-down blade built using 3D printing technology. This scaled-down model was examined experimentally and numerically to obtain dynamic characteristics then the measurements were used to predict the dynamic characteristics of 7 m long full-scale blade and validating its numerical model. Good agreement was found between the predictions of the full-scale blade and its numerical solutions. The second case was using the numerical model of scaled-down similitude of the full-scale blade. Tip deflection analysis and modal analysis were performed on the numerical model of similitude. Results were used to predict and validate the numerical solutions of the 7 m full-scale blade. Better agreement was obvious.

Keywords- Wind turbine blades, Dimensionless analysis, Buckingham π -theorem, Dynamic characteristics, Tip deflection, Modelling, 3D printing technology, Similitude theorem.

1. Introduction

The blades represent a vital component of any horizontal axis wind turbine due to their complexity, cost and significant effect on the efficient operation. During its lifetime, a wind turbine blade is subject to different types of loads; aerodynamic, inertial, and gravitational [1]. The designers aim at increasing the lifetime of wind turbine blades to exceed the 20 year life cycle, prescribed by most standards and international regulations, while subject to those complex mixture of static and dynamic loading.

Not only is the initial cost of blade considerable, but also the breakdown time and re-installation costs sometimes are even more expensive. This puts an increased demand on the

accurate tools needed to carry out performance characterization tests of the wind turbine blades prior to installations such as mechanical testing as stated in detail by IEC-61400, Part23 [2]

Testing of wind turbine blades prototypes can be categorized into static bending test to check the stiffness of the blade, fatigue test to check its durability to cyclic loads, and dynamic test to specify the natural frequencies of the blade [2]. Another tool exists, which is as important, namely pre-testing of the blade to estimate the structural and aerodynamic behaviours of the blade during the design stage for further modifications before manufacturing.

Pre-testing is usually based on developing the numerical models capable of simulating the behaviour of the blades under various load conditions. Along that track, extensive efforts have been implemented to establish a time- and cost-efficient methodology to numerically verify the performance of wind turbine blades.

The dynamic characteristics of horizontal axis wind turbine blade are important to ensure that the blade is rotating at frequencies as far as possible from its natural frequencies to prevent resonance phenomena. The tip deflection is important to ensure that the blade will not collide with the tower during rotation due to operational loads. This, of course in conjunction with the augmented effect of static and dynamic loads that would in some cases reach the blade to critical state due to the excessive combined loads.

Several researchers have acknowledged the importance of developing accurate numerical models for that particular reason, particularly with the increased demand on longer, heavier and more complicated designs of wind turbine blades.

Kevin Cox and Echtermeyerb [3] performed finite element studies on a 70m horizontal axis wind turbine blade to check its ability to survive extreme loads.

Tartibu et al [4] modelled a horizontal axis wind turbine blade approximately as stepped and uniform beams then determined the natural frequencies of these beams experimentally and numerically.

Xinzi et al [5] designed a numerical model for a 10KW horizontal axis wind turbine with fixed pitch and variable speed. The blade geometry was modelled in CATIA and the Finite Element Model (FEM) was developed using ABAQUS implementing linear model for blade materials. By using the FEM model, deflections and strain distributions of the blade under extreme wind conditions were numerically predicted. The results showed that the clearance between the blade tip and tower is sufficient to prevent collision and the blade material is linear.

Several researchers tried to verify the finite element model experimentally to ensure the validity of the model. Experimental tests are performed either on a full scale prototype of the blade or scaled down models.

Dhar [6] proposed a methodology to design a small-scale test set-up of a full-scale wind turbine. Dhar developed a finite element model of the full-scale wind turbine. His model was dimensionless to reach the structural invariants which were used to design the structural components of the small-scale test set-up.

Ridder et al [7] proposed a methodology to obtain the power and thrust coefficients of a scaled-down floating wind turbine model same as that of the full-scale wind turbine by modifying the geometry of the scaled down blades to provide thrust equality with the full-scale. After performing Computational Fluid Dynamics (CFD) analysis, they built a

scaled-down model with scale factor 1: 50 and successfully tested it.

Murugan et al [8] attempted to develop a scaling law procedure for models to carry out the free vibration analysis of structures, based on the scaled-down model requirement.

Kwon et al [9] investigated the performance tests of a scaled-down model of a 750 KW wind turbine with dimensional scale factor 1: 23. Structural performance tests were conducted on the scaled-down model using embedded Fibre Bragg Grating sensors (FBG). The results proved the reliability of evaluating structural behaviour of the composite blade during the performance tests using embedded Fibre Bragg Grating sensors (FBG) for full-scale blade.

Scaled-down structural models were built similar to the real structure but with suitable geometric scaling. The purpose of building scaled-down models differs from one researcher to another. It is sometimes used to merely demonstrate the shape of the full scale structure. In some cases, it is used to validate the numerical model by conducting tests on the scaled-down model and comparing with the predictions of the numerical one. In other cases, they are used to verify the manufacturing methods. Predicting the characteristic and performance of the full-scale blade from the scaled-down model is not at all a straightforward process.

The purpose of this paper is to introduce a new systematic approach to predict the static and dynamic structural responses of large wind turbine blades from scaled-down models. This developed approach is based on dimensionless analysis using the Buckingham π -Theorem to relate the scaled-down model to the full-scale blade.

The paper at hand is divided in 4 sections starting with an introduction, followed in section 2 with the Buckingham π -Theorem, where it is studied and implemented on wind turbine blades to develop a methodology predicting the static and dynamic relations between scaled-down and full-scale blades. In Section 3, the proposed methodology is tested and validated through the following steps:

- Manufacturing of an adequate scaled-down blade model (i.e. the dimension scale factor is uniform for most of geometrical dimensions) using 3D printing technology.
- Developing a finite element model for the adequate scaled-down blade to predict its dynamic performance.
- Measuring the natural frequencies of the adequate scaled-down blade and validating the outcomes of the corresponding finite element model.
- Developing a full-scale blade model of 7 m length.
- Applying the proposed methodology to predict the natural frequencies of the full-scale blade from those of the down-scaled one.
- Comparing the predictions of the proposed methodology with those of a finite element model for the full-scale blade.

➤ Developing another finite element model for the scaled-down blade as complete similitude of the full-scale blade (i.e. the dimension scale factor is uniform for all geometrical dimensions).

➤ Using the outcomes of the dynamic and static analysis of the scaled-down similitude blade to predict the dynamic and static responses of the full-scale blade.

➤ Comparing the predictions of the proposed methodology with those of the finite element model of the full-scale blade.

Section 4 concludes the outcomes of this research. The proposed methodology can be a very useful tool in the pre-testing of wind turbine blades accurately with low costs.

2. Theory of scaled down modelling

The geometric scaling by itself affects the structure behaviour including its static stiffness and dynamic characteristics and strength, etc. In order to consider the scaled down model as complete similitude to the prototype, then every variable affecting the behaviour of the scaled down model and the full scale structure must resemble a fixed ratio of their original counterparts in full-scale structures, which is called the Scale Factor [10].

Scaled-down models can be true, adequate, or distorted [11]. The true model is the one that represent the response of full- scale structure exactly. The adequate model is the one that provides good predictions for at least one characteristic of the full-scale structure. The distorted one is the one that mismatch the full-scale structure and violate some design conditions.

A dimensional analysis that correlates the performance of the scaled-down model and the full-scale structure is carried out, where the dimensional homogeneity is to be ensured followed by derivation of dimensionless groups of the variables that control the physical phenomena [12].

There are three basic methods to derive these dimensionless groups. The first method is by putting the governing equations in dimensionless forms and hence the dimensionless groups could be defined.

The second method is Buckingham π –Theorem, which states that any dimensional physical equations can be arranged as non-dimensional groups. Buckingham symbolized the dimensionless group with symbol “ π ” and the groups are referred to “ π groups” [13].

The third method is Rayleigh’s method. This method is valid only if the number of variables on which, physical phenomena under consideration depends is less than or equal to four. It becomes extremely difficult to apply that method if more variables are involved [14].

In this work, the Buckingham π –Theorem is applied to get dimensionless groups of the natural frequencies and the tip deflection under steady aerodynamic forces of the blades. The Buckingham π –Theorem is used when all influential quantities are known without the need of knowing the

governing mathematical equations. The derivation of the π –Theorem is demonstrated in many textbooks such as [15].

2.1. Application of Buckingham π –Theorem in dynamics

To demonstrate the adequacy and applicability of the proposed method, consider a physical phenomenon X that is function (f) of k variables such that,

$$X = f(x_1, x_2, x_3, \dots, x_k) \tag{1}$$

or,

$$f(X, x_1, x_2, x_3, \dots, x_{k-m}) = 0 \tag{2}$$

then we can write this function in dimensionless form as follows,

$$g(\pi_1, \pi_2, \pi_3, \dots, \pi_{k-m}) = 0 \tag{3}$$

where the number of π terms is equal to number of variables k minus the number of fundamental dimensions m involved in the analysis (e.g. mass M , length L , and time T).

A full explanation of the Buckingham π –Theorem can be found in [15]. In order to obtain the dimensionless groups representing the natural frequencies of the full scale blade, one has to define the variables affecting them.

Natural frequency f_n is influenced by elasticity modulus E , moment of inertia I , cross section area A , length L and material density ρ such that,

$$\varphi(f_n, E, I, A, L, \rho) = 0 \tag{4}$$

The dimensional form of the variables is presented in Table 1.

Table 1.The dimensional forms of the variables

Physical variable	Dimensional form
f_n	T^{-1}
E	$M L^{-1} T^{-2}$
I	L^4
A	L^2
L	L
ρ	$M L^{-3}$

The repeating variables are the ones which repeat in each π term analysis. They have been chosen based on the following selection criteria [16];

- They do not form dimensionless formulation when they combined.
- After combining them, they include all the dimensions.
- They can be measured experimentally.
- They describe material and geometrical properties.

Therefore, the repeating variables are (f_n, L and ρ).

The non-repeating variables each one of them will appear in a π term. The non-repeating variables are (E, I and A).

The number of variables, $k = 6$.

The number of dimensions, $m = 3$.

So the number of dimensionless π terms $k - m = 6 - 3 = 3$ groups.

The first π term is formulated by putting the repeating variables (f_n, L and ρ) with exponents (a, b , and c) respectively such that,

$$\pi_1 = f_n^a \cdot \rho^b \cdot L^c \cdot E \quad (5)$$

To ensure the right hand side is non-dimensional, the exponents of all dimensional variables should be equal to zero. Therefore,

$$M^0 L^0 T^0 = (T^{-a}) \cdot (M^b L^{-3b}) \cdot (L^{-c}) \cdot (M L^{-1} T^{-2}) \quad (6)$$

yielding,

$$M: 0 = b + 1 \quad (7)$$

$$L: -3b - c - 1 = 0 \quad (8)$$

$$T: 0 = -a - 2 \quad (9)$$

then, $a = -2, b = -1$, and $c = -2$

and,

$$\pi_1 = E / (f_n^2 \cdot \rho \cdot L^2) \quad (10)$$

The second π group is formulated such that;

$$\pi_2 = f_n^a \cdot \rho^b \cdot L^c \cdot A \quad (11)$$

then, the exponents of all dimensional variables should be equal to zero therefore,

$$M^0 L^0 T^0 = (T^{-a}) \cdot (M^b L^{-3b}) \cdot (L^{-c}) \cdot L^2 \quad (12)$$

yields, $a = b = 0$ and $c = -2$

therefore;

$$\pi_2 = A / L^2 \quad (13)$$

The third π group is formulated as follows:

$$\pi_3 = f_n^a \cdot \rho^b \cdot L^c \cdot I \quad (14)$$

$$M^0 L^0 T^0 = (T^{-a}) \cdot (M^b L^{-3b}) \cdot (L^{-c}) \quad (15)$$

yielding, $a = b = 0$ and $c = -4$ after equating the exponents with zero therefore;

The third π group is formulated as follows;

$$\pi_3 = I / L^4 \quad (16)$$

2.2. Application of Buckingham π -Theorem in estimating the tip deflection under aerodynamic forces analysis

The tip deflections δ under steady aerodynamic forces are affected by transverse force P , elasticity modulus E , moment of inertia I , and length of the blade L such that,

$$\varphi(\delta, E, I, L, P) = 0 \quad (17)$$

The dimensional forms of the variables are listed in Table 2.

Table 2. The dimensional forms of the variables

Physical variable	Dimensional form
δ	L
E	$M L^{-1} T^{-2}$
I	L^4
L	L
P	$M L T^{-2}$

The number of variables, $k = 5$.

The number of dimensions, $m = 2$.

So the number of dimensionless pi groups = $k - m = 5 - 2 = 3$ groups.

The repeating variables are (L and E).

The non-repeating variables are (δ, P and I).

The first π group is formulated such that;

$$\pi_1 = \delta \cdot E^a \cdot L^b \quad (18)$$

$$M^0 L^0 T^0 = L^1 \cdot (M L^{-1} T^{-2})^a \cdot L^b \quad (19)$$

then, $a = 0$ and $b = -1$

yielding,

$$\pi_1 = \delta / L \quad (20)$$

The second π group is formulated as follows;

$$\pi_2 = P \cdot E^a \cdot L^b \quad (21)$$

$$M^0 L^0 T^0 = (M L T^{-2}) \times (M L^{-1} T^{-2})^a \times L^b \quad (22)$$

then, $a = -1$ and $b = -2$

yielding,

$$\pi_2 = P / (E \cdot L^2) \quad (23)$$

$$\pi_3 = I \cdot E^a \cdot L^b \quad (24)$$

$$M^0 L^0 T^0 = (L^4) \cdot (M L^{-1} T^{-2})^a \cdot L^b \quad (25)$$

yielding, $a = 0$ and $b = -4$ hence,

$$\pi_3 = I/L^4 \quad (26)$$

3. Verification of the proposed methodology

The proposed methodology is validated through several steps. The procedure for this validation process is demonstrated in Fig.1. As shown in the Fig.1. the validation process starts by designing a full-scale blade. The chosen blade is then scaled down to a smaller model which is designed and manufactured using 3D printing technology. The scaled-down design is examined numerically (using the Finite Element method) and the 3D printed model is examined experimentally.

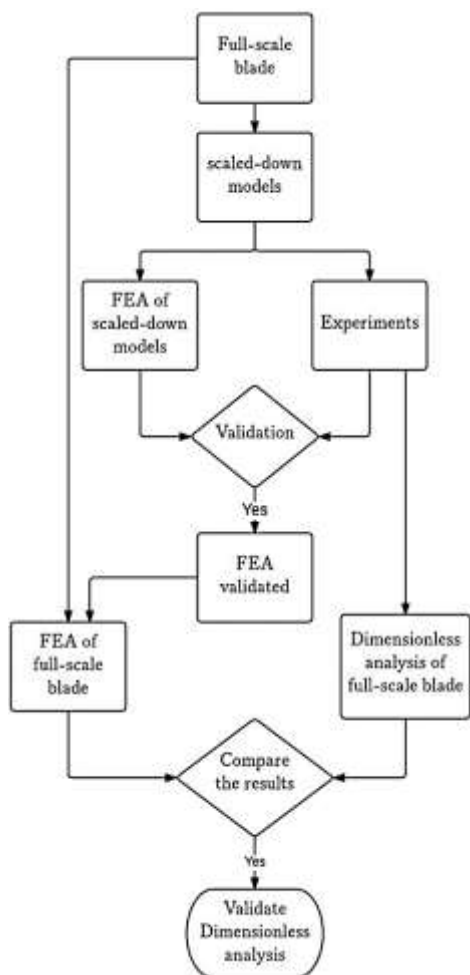


Fig. 1. The validation process chart

The results from the numerical model and experimental measurements are compared together. Once validated, the Finite Element model is used to analyze the full scale blade to predict its behavior.

On the other hand, the proposed dimensional analysis methodology is used to predict the behavior of the full scale blade from the measurements and Finite Element Analysis of the scaled down model.

The predictions of the dimensional analysis model are compared to those of the Finite Element model which is already validated. Hence, the proposed dimensional analysis model is validated.

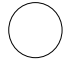


The rest of this section provides the details of the work carried out within this verification process.

3.1. The full-scale blade Design

To verify the proposed methodology, it is applied to a 7 m long full-scale wind turbine blade. The blade geometry was created using SolidWorks program. The basic aero foil chosen for the blade is FFA-W series which developed by the Aeronautical Research Institute of Sweden. The transition between sections is obtained by linear interpolation.

The properties of the aero foils are listed in Table 3. The aerodynamic design of the full-scale blade is provided in the appendix.

Table 3. The configuration of aero foils along the blade where R is the radius of the turbine

Aero foil Type	Aero foil Shape	Station
Circle		$(0.0358).R$
Transition from root to FFA-W3-301		$(0.10. - 0.25).R$
Linear transition from FFA-W3-301 to FFA-W3-211		$(0.26 - 1).R$

The structural design of the blade should be capable of showing good bending and torsional stiffness under the operational loads. The outer body of the blade is divided to two sides, pressure and suction sides. The outer body is formed from composite material plies. To increase rigidity of the blade, spar is inserted inside the blade. The common types of the spar are one, two shear webs, and box girder [17]. Two shear webs are inserted in the 7 m long blade as shown in Fig.2.

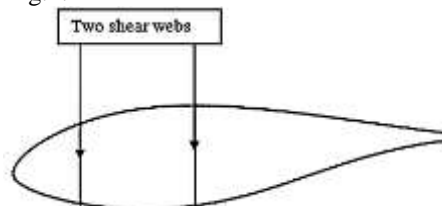


Fig. 2. The schematic drawing of the cross-section of aerofoil of the full-scale blade

The material of this 7 m blade is glass fibers reinforced epoxy composite, with 55% fiber volume ratio. It is common to use fiber glass epoxy composite plies as they have been reported to show high strength to weight ratio [18].

Ply of unidirectional (UD) glass-epoxy composite are used but with different orientations to the fibers in order to withstand bending in flap wise direction and torsional stress. The fibers are oriented in the plies with angles $0^\circ/\pm 45^\circ$ as this is the most common layup [3].

The 0° fiber orientation of the fibers where fibers are parallel to the shear webs, contributes in increasing stiffness in the flap wise direction against the bending and the $\pm 45^\circ$ fiber orientation contributes in resisting torsion and hence increasing the torsional stiffness [19], the layup is shown in Fig. 3.

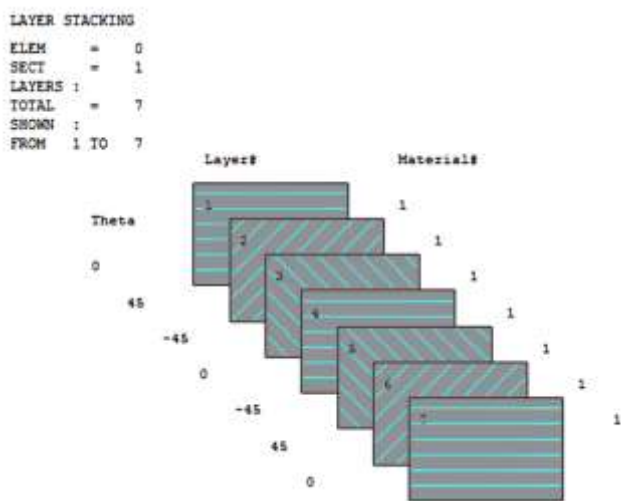


Fig. 3. Layup of the GFRP composite plies

The properties of the UD glass fiber reinforced epoxy are presented in Table 4.

Table 4. Mechanical properties of GFRP, source [20]

Property	Value
E_1 (GPa)	41
E_2 (GPa)	9
E_3 (GPa)	9
G_{12} (GPa)	4.1
G_{13} (GPa)	4.1
G_{23} (GPa)	3.3
ν_{12}	0.3
ν_{13}	0.3
ν_{23}	0.35
ρ (kg/ m ³)	1890

3.2. The Scaled-down model

The 7m long blade was scaled down to 0.3 m length. The dimension scale factor between the reduced and the full-scale models is denoted by S and it equals to $(0.3/7)$. The scaled-down model was manufactured by fused

deposition modeling (FDM) which is one of rapid prototyping technologies [21] using 3D printing machine Dimension BST 768, shown in Fig.4.



Fig. 4. 3D Printer, Dimension bst 768

The specifications of the 3D printer machine are listed in Table 5.

Table 5. The specifications of the 3D printer machine

Machine Type	Dimension BST 768
Maximum size of printed part	203 × 203 × 305 mm
Model material	ABS-plus (Acrylonitrile Butadiene Styrene)

The blade geometrical model was developed in SolidWorks environment then converted to STL format and provided to the machine core software (Catalyst EX).

The model material is ABS plus-Plastic. Model material was extruded from the cartridge in the 3D printing machine line by line to create a layer and hence building the whole geometry of the scaled-down blade layer by layer.

Figure 5 shows the adequate scaled-down model built by 3D printing method.



Fig. 5. The scaled-down 3D printed model.

The thickness of the aero foils of the scaled-down blade was not scaled according to the dimension scale factor S because of manufacturing constraints but the other parameters of blade were scaled uniformly according to S .

This scaled-down blade is considered as adequate model. Meanwhile, a numerical model of the scaled-down blade was developed using ANSYS APDL.

The scaled-down blade was examined experimentally to validate the numerical solutions.

3.3. Experimental Methodology of Natural Frequencies determination

Two common techniques are usually used to apply dynamic loading on structures either by using an electromagnetic shaker or by using an impact hammer.

The first method was selected in which the blade is fixed to the shaker oscillating head, which is excited by an amplified white noise signal. The reasons behind using an electromagnetic shaker testing instead of impact hammer are:

- Different excitation types of signals can be applied such as White Noise, Sine Sweep, Etc.
- The 3D printed blade may fail under improper impact force.

3.3.1. The Test Apparatus

1. Accelerometer

Model 352A21PCB, from PIEZOTRONIC Company,
 Lightweight (0.6 gm) ceramic shear type 10 mV/g, 1 to 10k Hz

2. Signal Function Generator

Model DS360, Ultra low distortion

3. Shaker

Inertia type IV-40 manufactured by Data Physics.

4. Data Acquisition system

LMS-SCADAS mobile data acquisition

5. Power Amplifier

Model PA100E manufactured by Data Physics

The layout of the experiment is given in Fig. 6. The measurements are performed in two directions flap wise and edge wise.

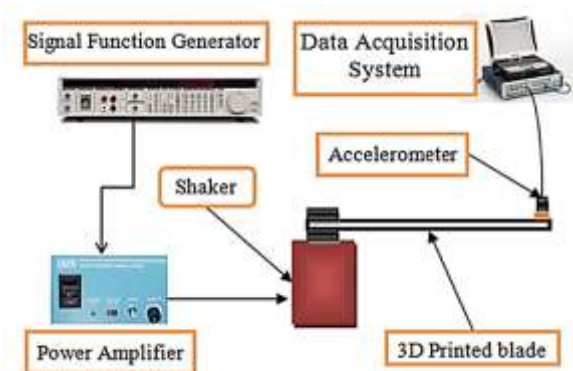


Fig. 6. The layout of the experiment

Figure 7 shows the fixation of the blade and the accelerometer put on the flap wise direction.

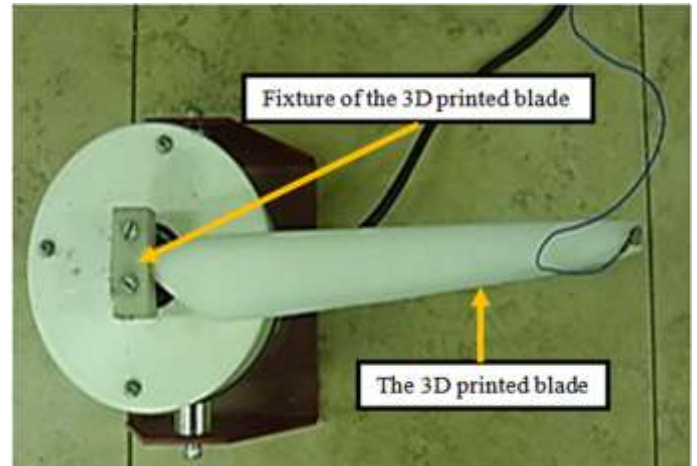


Fig. 7. The experimental modal analysis in flap wise direction

Figure 8 shows the case of extracting natural frequencies of the blade in edge wise direction.

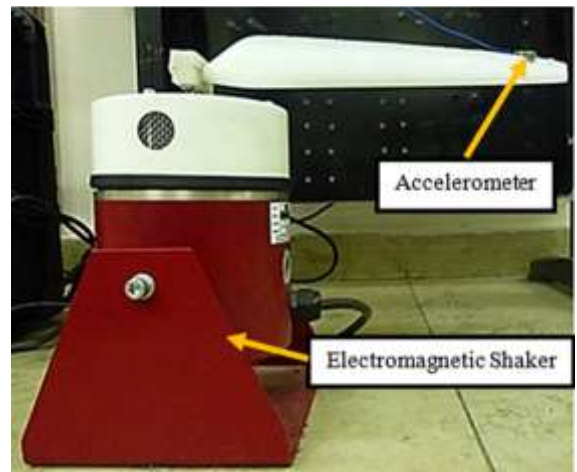


Fig. 8. The experimental modal analysis in edge wise direction

Figure 9 shows the measured tip acceleration at range of frequencies of the white noise excitation in the flap wise.

Figure 10 shows the natural frequencies in edge wise direction of the blade.

The peaks in fig.9 and fig.10 are corresponding to the natural frequencies of the blade.

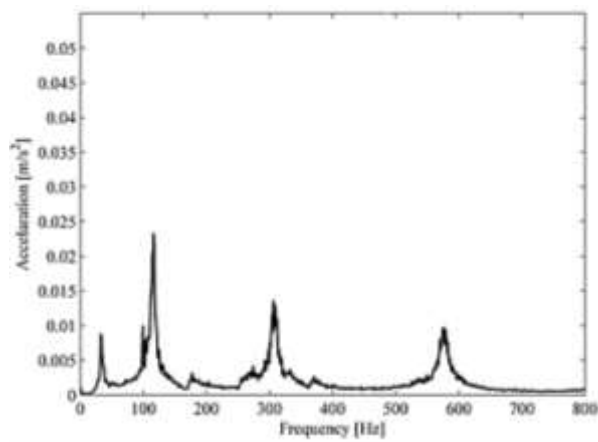


Fig. 9.Frequency against acceleration FFT graph in flap wise direction

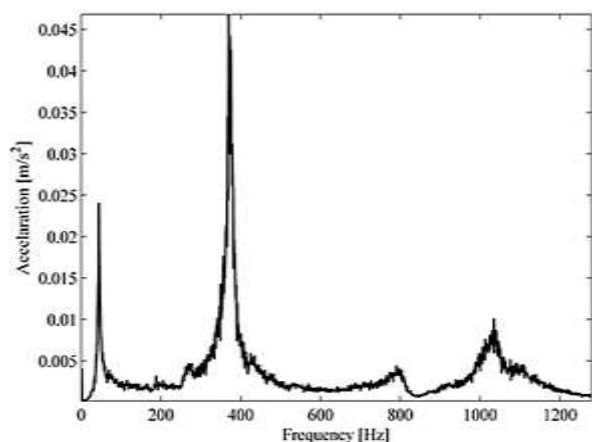


Fig. 10.Frequency against acceleration FFT graph in edge wise direction

Table 6 summarizes the results in each direction.

Table 6.The Natural frequencies computed using MATLAB code

Mode Number	Frequency (Hz)	
	Flap wise Direction	Edge wise Direction
1	32.5	44.38
2	116.3	370
3	306.3	-

3.3.2. The finite element analysis of the scaled-down model

The blade was analyzed using ANSYS APDL 14.5 with SHELL element type SHELL181. The blade was manufactured as layers with thickness of 0.254 mm by 3D printer machine. An orthotropic material model is considered.

The elastic tensile moduli in longitudinal E_x , and transverse directions E_y , and the density ρ were determined experimentally by researchers on the track to analyze fatigue

characteristics of wind turbine blades. The experiments were performed on a uniform rectangular beam and then measuring its natural frequencies in the longitudinal and transverse directions.

The measured natural frequencies were used in the equation of the natural frequency and then the elasticity moduli were extracted. The mass of the uniform beam was measured using a sensitive scale and then multiplied by the volume consequently the density was computed. The other 6 independent elastic constants (G_{xy} , G_{yz} , G_{xz} , ν_{xy} , ν_{yz} , and ν_{xz}) were taken from study of Mamadapur [21] on the parts manufactured by 3D printing technique. The mechanical properties of the material are listed in Table 7. The mesh density was globally specified in mesh tool window. Using SIZE input parameter for the element, the element edge size is 0.0018 m yielding 9628 elements. SIZE parameter helps in generating a mesh with all elements having edge sizes as close as possible to the specified value [22].

Table 7.The mechanical properties of the ABS-plus plastic blade

Property	Value
E_x (GPa)	1.09
E_y (GPa)	1.05
E_z (GPa)	1.05
ν_{xy}	0.39
ν_{yz}	0.37
ν_{xz}	0.37
G_{xy} (GPa)	0.676
G_{yz} (GPa)	0.645
G_{xz} (GPa)	0.645
ρ (kg/ m ³)	960

The FEM meshed model of the scaled down blade is shown in Fig. 11. There are 6 Eigen solver methods in ANSYS modal analysis to extract mode shapes. The most common method is Block Lanczos because it is a fast efficient solver [23]. Additionally this method is suitable for shell models.

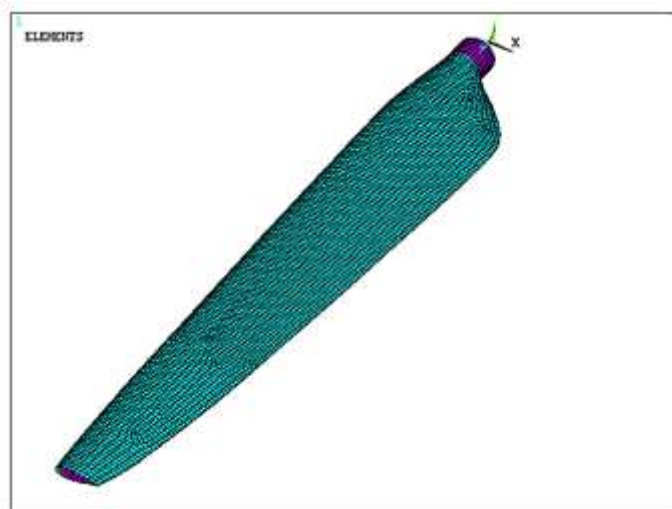


Fig. 11.The meshed blade

3.4. Discussion of results of the experimental and FEM pre-test of the scaled down model

The results of the FE modeling are validated by the measurements. The results for flap wise direction are convergent. A higher error is witnessed in the third mode calculation because the higher modes are sensitive to shape of elements. Table 8 shows comparison between the measurements and the FE results. The results in edge wise direction shows appropriate convergence for first mode and higher convergence in the second mode as clear in Table 8.

The edge wise direction is stiffer than the flap wise one because the chord length is larger than the thickness of the aerofoil so the moment of inertia is higher in that direction than in flap wise direction.

The first two mode shapes in edge wise direction are investigated just to verify the approach as it is not expected for a blade during its lifetime to reach such rotational frequencies.

Figure 12 shows the different mode shapes in flap wise and edge wise directions of the scaled-down model

Table 8. The comparison of computed natural frequencies to the experimental results of adequate scaled-down blade

Mode Number	Flap wise direction			Edge wise direction		
	Experimental results (Hz)	FE results (Hz)	Error (%)	Experimental results (Hz)	FE results (Hz)	Error (%)
1	32.5	32.59	-0.28	44.38	52.78	-19
2	116.3	118.43	-1.8	370	377.14	-1.9
3	306.3	274.1	10.5	-	-	-

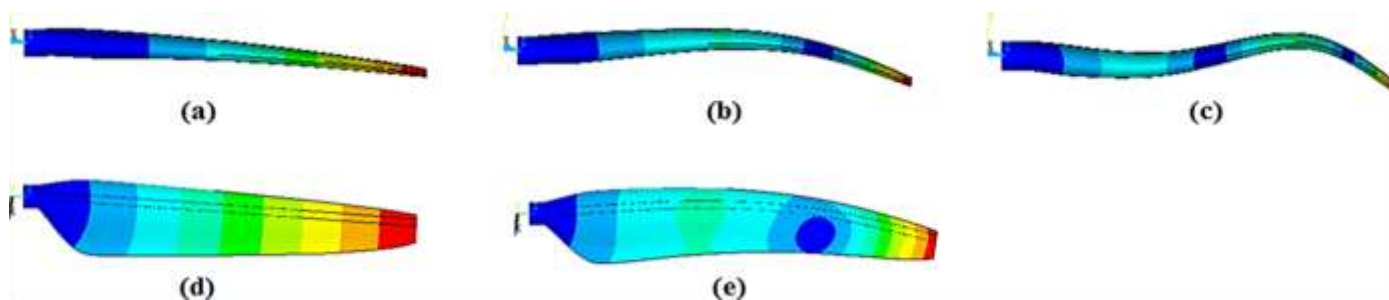


Fig. 12. The mode shapes of the scaled down numerical model; (a),(b) and (c) represent the first 3 mode shapes in flap wise direction; (d) and (e) represent the first two mode shapes in edge wise direction

The mass of the blade in the analysis is 0.0352 Kg, but using the sensitive scale, the actual mass of the blade is 0.02953 Kg. The difference is attributed to voids between some layers created during the depositing process of the blade that reduces the shear strength and the mass of the actual blade compared to the FE model.

3.5. Finite Element modeling of the full-scale blade

Analytical modal analysis was performed on the full-scale blade to extract the natural frequencies and later, these results will be compared with the predicted values by using the Buckingham π -Theorem relations to verify its applicability in that field.

The blade surface model is imported in a para solid model format to ANSYS APDL 14.5 software. The plies of the composites were 7 plies each of 0.001 m thickness. SHELL elements are used to simulate the composite layout of the blade as they are easy to set up and modify lays [24].

The element SHELL181 is chosen from ANSYS Element Library to simulate the composite layer structure of the blade surface. SHELL181 is suitable for analyzing thin to moderately-thick shell structures.

The element is a 4-node with 6 degrees of freedom per node, translations in the x, y, and z directions, and rotations about the x, y, and z-axes [25]. The minimum length of element edge was 0.025 m. The total number of elements is 21,773 elements.

The mesh is uniform with elements of edge size as close to the specified as possible.

A modal analysis was conducted and the results are listed in Table 9.

Table 9. Summary of the results of FE modal analysis on the 7m blade

Mode Number	Frequency (Hz)	
	Flap wise Direction	Edge wise Direction
1	5.60	7.45
2	23.61	66.15
3	50.31	-

3.5.1. Prediction of the Natural frequencies of the 7-m blade

In order to match the physical relations between the scaled down model and the full-scale structure, the π groups must be the same for the model and the real structure,

$$\pi_{\text{scaled-down model}} = \pi_{\text{full-scale structure}} \quad (27)$$

$$E_s / (f_{ns}^2 \cdot \rho_s \cdot L_s^2) = E_r / (f_{nr}^2 \cdot \rho_r \cdot L_r^2) \quad (28)$$

Subscripts s and r refer to the scaled-down model and the full-scale structure respectively.

The following assumptions are considered during using Buckingham π – Theorem:

- For the full-scale blade, in plane longitudinal elasticity modulus E_1 is larger than the transverse E_2 and perpendicular elasticity moduli E_3 so it is only considered in the equations.
- The blade is treated as Euler-Bernoulli beam.

Eq. (10) is arranged such that,

$$f_{nr} = f_{ns} \cdot \left(\frac{L_s}{L_r} \right) \cdot \sqrt{(E_s \cdot \rho_s) / (E_r \cdot \rho_r)} \quad (29)$$

By substituting of the experimental natural frequencies of the scaled-down blade in Eq. (29), the natural frequencies of the full-scale blade were computed. Table 10 provides comparison between the finite element results and the predicted results for the full-scale blade.

Table 10. The comparison between predicted natural frequencies and the FE results for the full-scale blade

Mode Number	Flap wise direction			Edge wise direction		
	Prediction of full-scale natural frequency (Hz)	FE results (Hz)	Error (%)	Prediction of full-scale natural frequency (Hz)	FE results (Hz)	Error (%)
1	6.06	5.6	7.6	8.20	52.78	9.14
2	21.71	23.61	-8.7	69.10	66.15	4.26
3	57.2	50.31	12.04	-	-	-

Mean Absolute Deviation (*MAD*) is used to measure the closeness of the predicted results p_i to the numerically solved results r_i as clear in Eq. (30). Furthermore, *MAD* is a good technique to compare between different methods therefore it will be used to compare between using full similitude scaled-down model and adequate scaled-down model as clear in section 3.6.1.

$$MAD = \frac{1}{n} \cdot \sum_{i=1}^n |p_i - r_i| \quad (30)$$

where n is the number of measurements (i.e. $n = 5$)

The *MAD* of the results of the full-scale blade is equal to 2.59.

The discrepancies between the predicted and FE results of the full-scale blade are attributed to:

- The small influence of transverse and perpendicular elasticity moduli E_2 and E_3 which is not considered.
- The layup of the adequate scaled-down blade model is not similar to the layup of the full-scale blade which affects the predicted frequencies of the full-scale blade.
- The potential error associated with the numerical solutions.

3.6. The numerical scaled-down complete similitude model

3.6.1. The natural frequencies predictions for the full-scale blade

In order to have a better predictions of the full scale blade, the scaled-down model should be a full similitude for the full-scale blade (i.e. the dimension scale factor is constant for the whole geometry). In this section, a modal analysis was conducted to this scaled-down numerical model whose length is 0.3 m and its layer thickness of 0.00029 m as described previously in section 3.3.2. The results of the modal analysis of the scaled-down similitude are tabulated in table 11.

Table 11. Results of FE modal analysis on the scaled-down similitude

Mode Number	Frequency (Hz)	
	Flap wise Direction	Edge wise Direction
1	30.74	43.12
2	129.64	345.78
3	284.67	-

The natural frequencies of the scaled-down similitude were used in Eq. (29) therefore the natural frequencies of the full-scale blade were calculated. Table 12 shows comparison

between the predicted frequencies of the full-scale blade and its finite elements results. A better agreement between predicted and numerical results is obvious.

Table 12.The comparison between predicted natural frequencies and FE results of the full-scale blade

Mode number	Flap wise direction			Edge wise direction		
	Prediction of full-scale natural frequency (Hz)	FE natural frequency (Hz)	Error (%)	Prediction of full-scale natural frequency (Hz)	FE natural frequency (Hz)	Error (%)
1	5.74	5.60	2.44	8.05	7.45	7.45
2	24.20	23.61	2.43	64.58	66.15	-2.43
3	53.15	50.31	5.34	-	-	

The mean absolute deviation is equal to 1.148. It is less than that of the adequate scaled-down model by the half approximately. Therefore, method of using complete scaled-down similitude is better because it has lower MAD.

3.6.2. Predictions of deflection of the full-scale blade

The stiffness of the blade must be ensured to survive the operating loads. A computational fluid dynamics (CFD) analysis was performed on the blade using an open source code called Open FOAM.

The analysis showed that the maximum normal force occurs at wind speed of 10.5 m/s with magnitude of 2600 N and the tangential force with magnitude 475 N. It is obvious that this load is much smaller and is acting along the stiffer direction of the blade and hence the flap wise load case is more crucial because it causes deflection of the blade that reduces the clearance between the blade and the tower.

A structural performance analysis was performed on the full-scale blade to compute its deflection per unit force at the tip in flap wise and edge wise directions. Each force was put on the tip of the full-scale blade separately to check the maximum deflection of the blade. The numerical static structural analysis was performed on the scaled-down similitude model.

Eq. (23) is rewritten as clear in Eq. (31) to scale the aerodynamic forces on the full-scale blade then put on the tip of the scaled-down similitude each separately in flap wise and edge wise directions.

$$P_f / (E_f \times L_f^2) = P_s / (E_s \cdot L_s^2) \quad (31)$$

The tip deflection of the scaled-down similitude is used to predict the tip deflection of the full-scale blade using Eq. (32).

$$\delta_s / L_s = \delta_f / L_f \quad (32)$$

Furthermore, the relation between various forces and the associated deflections is linear as the deflection per unit force is approximately constant for different set of measurements on flap wise and edge wise directions.

Table 13 shows comparison between predicted full-scale deflection per force and the FE solutions.

Table 13.The comparison between predicted tip deflections of the 7m blade and its FE results

FE result of similitude blade deflection per force (mm/N)	Prediction of full-scale blade deflection per force (mm/N)	FE result of full-scale blade deflection per force (mm/N)
Flap wise direction		
25.55	0.0288	0.0254
Edge wise direction		
10.34	0.0117	0.0104

Meanwhile, the gravitational force is the main source of bending on the edge wise direction and this load is causing cyclic moment at the root [26].

The maximum value of the weight occurs when the axis of the blade is horizontal however the deflections due to gravitational force are not included in the study because the deflections vary cyclically according to position of the blade and the research concerns with the static tip deflection due to aerodynamic forces.

The differences between the tip deflection in the flap wise and edge wise directions predicted from the scaled-down similitude results and the FEM results of the full scale blade are attributed to:

- The layup of the scaled-down similitude layers is not similar to that of the full scale blade
- The material dissimilarities effects
- The geometrical complexity effects
- The potential error associated with numerical solutions

4. Conclusion

The Buckingham π -Theorem is adapted to predict the behaviour of full scale wind turbine blades from scaled down models. The dimensionless analysis using Buckingham π -Theorem is done to obtain dimensionless groups for correlating the static and dynamic behaviours of the scaled-down model to those of the full-scale blade. The 3D printing technique is a reliable method for building scaled-down models.

Two different scaled-down models are used to predict the behaviour of a 7 m full-scale blade. Adequate scaled-down model and scaled-down similitude model.

The experimental natural frequencies of the adequate scaled-down model are used in the dimensionless equation to predict those of the full-scale blade. The modal analysis is performed on the full-scale blade numerical model.

Appropriate agreement was shown between the numerical solutions and predicted solutions of the full-scale blade.

The second scaled-down model is the numerical scaled-down complete similitude. Modal analysis is performed on the numerical scaled-down complete similitude and consequently the natural frequencies are used to predict the natural frequencies of the full-scale prototype. The predicted natural frequencies of the full-scale blade showed better agreement with the numerical solutions. The mean absolute deviation is computed for the two cases to compare between them and the complete similitude model is found to be better because it shows lower mean absolute deviation. Numerical structural analysis is performed on the full-scale blade and the scaled-down similitude model.

The normal and tangential aerodynamic forces are scaled according to Buckingham π -Theorem dimensionless groups. The scaled normal force is applied on the tip in flap wise direction of the similitude model and the scaled tangential force is applied on the tip in the edge wise direction.

The tip deflection per unit force of the scaled-down similitude is computed. Through dimensionless groups, the tip deflection per unit force of the full-scale blade is calculated. Subsequently the predicted tip deflection per unit force of the full-scale blade is compared with its numerical solution.

The results show good agreement to some extent between the predicted values and the FE ones especially in the edge wise directions.

The results show that the scaled-down models are suitable for predicting the dynamic characteristics and tip deflection of the full-scale blade therefore any modifications can be implemented during the design stage of the full-scale blades. The method of rapid prototyped scaled-down model of a full-scale blade proves to be a promising tool in the field of pre-testing and designing the horizontal axis wind turbine blades.

Acknowledgements

This study is carried out within the project entitled "Innovative Techniques for Design and Manufacturing of Wind Turbine Blades" funded by the Science and Technology for Development Fund (STDF) in Egypt. The aerodynamic design and forces of the full-scale blade are provided by Dr. Basman Elhadidi, Cairo University, Egypt.

Appendix

The geometry properties of the full-scale blade

Radius	Pre-Twist	Chord	Thickness	Thick%
(m)	(degree)	(m)	(m)	(t/c)
0.363	9.53	0.315	0.300	95.2
0.588	9.53	0.482	0.300	62.2
0.813	9.53	0.671	0.298	44.5
1.038	9.53	0.803	0.296	36.9
1.263	9.53	0.879	0.293	33.4
1.488	9.53	0.918	0.289	31.5
1.713	9.53	0.935	0.283	30.3
1.938	9.53	0.939	0.276	29.4
2.163	8.98	0.935	0.267	28.6
2.388	8.73	0.927	0.258	27.8

2.613	8.49	0.914	0.247	27.0
2.838	8.26	0.900	0.236	26.3
3.063	8.03	0.883	0.225	25.5
3.288	7.80	0.865	0.214	24.7
3.513	7.57	0.845	0.177	21.0
3.738	7.35	0.824	0.173	21.0
3.963	7.12	0.802	0.169	21.0
4.188	6.89	0.780	0.164	21.0
4.413	6.66	0.756	0.159	21.0
4.638	6.44	0.731	0.154	21.0
4.863	6.21	0.705	0.148	21.0
5.088	5.98	0.679	0.143	21.0
5.313	5.75	0.651	0.137	21.0
5.538	5.53	0.622	0.131	21.0
5.763	5.30	0.592	0.124	21.0
5.988	5.08	0.561	0.118	21.0
6.213	4.86	0.529	0.111	21.0
6.438	4.63	0.496	0.104	21.0
6.663	4.42	0.461	0.097	21.0
6.888	4.20	0.425	0.089	21.0

References

- [1] M. O. L. Hansen, *Aerodynamics of Wind Turbines*, London, England: Earthscan, 2008.
- [2] *Wind Turbine Generator Systems - Part 23: Full Scale Structural Testing of Rotor Blade*, 2001.
- [3] K. Cox and A. Echtermeyerb, "Structural design and analysis of a 10MW wind turbine blade," *Energy Procedia*, vol. 24, no. 2012, pp. 194-201, January 2012.
- [4] T. Kwanda, M. Kilfoil and A. Van der Merwe, "Vibration Analysis of a Variable Length Blade," *International Journal of Advances in Engineering & Technology (IJAET)*, vol. 4, no. 1, pp. 630-639, 2012.
- [5] X. Tang, R. Peng, X. Liu and A. I. Broad, "Design and Finite Element Analysis of Mixed Aerofoil Wind Turbines Blades," in *7th PhD Seminar on Wind Energy in Europe*, Delft, Netherlands, 2011.
- [6] Sandeep Dhar, *Development and Validation of Small-scale Model to Predict Large Wind Turbine Behavior*, Texas, USA, 2006.
- [7] E. J. de Ridder, W. Otto, G. Vaz, F. Huijs and G. J. Zondervan, "Development of a Scaled-Down Floating Wind Turbine for Offshore Basin Testing," in *33rd International Conference on Ocean, Offshore and Arctic Engineering*, San Francisco, 2014.
- [8] M. Ramu, P. V. Raja and P. R. Thyla, "Establishment of Structural Similitude for Elastic Models and Validation of Scaling Laws," vol. 17, no. 1, pp. 139-144, 2013.
- [9] B. Kwon, S. W. Kim, E. H. Kim, M. S. Rim, P. Shrestha and I. Lee, "Structural Performance Tests of Down Scaled Composite Wind Turbine Blade using Embedded Fiber Bragg Grating Sensors," *The International Journal of Aeronautical and Space Sciences (IJASS)*, vol. 12, no. 4, p. 346-353, 2011.
- [10] A. Williams, *Structural Analysis: In Theory and Practice*, Butterworth-Heinemann, 2009, pp. 381-382.
- [11] D. Fertis G, *Mechanical and Structural Vibrations*, New York: John Wiley & Sons, 1995, pp. 693-694.
- [12] C. Dym L and H. E. Williams, *Analytical Estimates of Structural Behavior*, New York, UK: Taylor & Francis, 2012, pp. 9-14.

- [13] C. Dym L, Principles of Mathematical Modeling, United States : Academic Press, 2004, pp. 24-25.
- [14] P. Balachandran, Engineering Fluid Mechanics, Delhi: PHI Learning Pvt. Ltd., 2013, p. 593.
- [15] J. Kuneš, Similarity and Modeling in Science and Engineering, Plzeň, Czech Republic: Cambridge International Science Publishing, 2012, p. 36.
- [16] U. Otey, Mechanics of Fluids, Bloomington, USA: AuthorHouse, 2008, p. 287.
- [17] M. Tarfaoui and O. R. Shah, "Spar Shape Optimization of a Multi-megawatt Composite Wind Turbine Blade," *Modal Analysis, Recent Advances in Composite Materials for Wind Turbines Blades*, pp. 93-104, 2013.
- [18] B. Eker, A. Vardar and A. Akdogan, "Using of Composite Material in Wind Turbine Blades," *Applied Science*, no. 6, pp. 2917-2921, 2006.
- [19] Ole Thybo Thomsen, "Sandwich Materials for Wind Turbine Blades Present and Future," *Sandwich Structures and Materials*, pp. 7-26, 2009.
- [20] J. Höyland, *Challenges for large wind turbine blades*, Trondheim, 2010, p. 64.
- [21] M. S.Mamadapur, *Constitutive Modelling Of Fused Deposition Modeling ACRYLONITRILE BUTADIENE STYRENE (ABS)*, Texas, 2007, p. 67 .
- [22] E. Madenci and I. Guven, *The Finite Element Method and Applications in Engineering Using ANSYS*, Arizona: Springer Science AND Business Media, LLC, 2006.
- [23] E. Wang and T. Nelson, "Structural Dynamic Capabilities of ANSYS," in *ANSYS*, Pittsburg,Pensylvania, 2002.
- [24] Z. Li, C. Li, W. Gao and Y. Wu, "Effect of Layup Design on properties of Wind Turbine blades," *Frontiers of Engineering Mechanics Research*, vol. 2, no. 3, pp. 63-70, August 2013.
- [25] ANSYS APDL, *Shell 181*, Pennsylvania: ANSYS .
- [26] V. Kumar Singh, T. Thomas T and V. Warudkar, "Structural Design of a Wind Turbine Blade: A review," in *International Conference on Global Scenario in Environment & Energy*, Bhubal, 2013.